

AN ECLIPSING MILLISECOND PULSAR WITH A POSSIBLE MAIN-SEQUENCE COMPANION IN NGC 6397

N. D'AMICO,^{1,2} A. POSSENTI,¹ R. N. MANCHESTER,³ J. SARKISSIAN,⁴ A. G. LYNE⁵ AND F. CAMILO⁶

¹Osservatorio Astronomico di Bologna, Via Ranzani 1, 40127 Bologna, Italy

²Istituto di Radioastronomia del CNR, Via Gobetti 101, 40126 Bologna, Italy

³Australia Telescope National Facility, CSIRO, PO Box 76, Epping, NSW 2121, Australia

⁴Australia Telescope National Facility, CSIRO, Parkes Observatory, PO Box 276, Parkes, NSW 2870, Australia

⁵University of Manchester, Jodrell Bank Observatory, Macclesfield, Cheshire SK11 9DL, UK

⁶Columbia Astrophysics Laboratory, Columbia University, 550 West 120th Street, New York, NY 10027

Received by ApJ Letters on 31 July, 2001

ABSTRACT

We present the results of one year of pulse timing observations of PSR J1740–5340, an eclipsing millisecond pulsar located in the globular cluster NGC 6397. We have obtained detailed orbital parameters and a precise position for the pulsar. The radio pulsar signal shows frequent interactions with the atmosphere of the companion, and suffers significant and strongly variable delays and intensity variations over a wide range of orbital phases. These characteristics and the binary parameters indicate that the companion may be a bloated main-sequence star or the remnant (still filling its Roche lobe) of the star that spun up the pulsar. In both cases, this would be the first binary millisecond pulsar system with such a companion.

Subject headings: globular clusters: individual (NGC 6397) — pulsars: individual (PSR J1740–5340) — binaries: close

1. INTRODUCTION

The millisecond pulsar J1740–5340 in the globular cluster NGC 6397 (D'Amico et al. 2001) is a member of a binary system with a relatively wide orbit of period 1.35 days, a companion with mass $M_c > 0.19 M_\odot$, and is eclipsed for about 40% of its orbit at a frequency of $\nu = 1.4$ GHz. In much tighter eclipsing binaries, like those containing PSRs B1957+20 (Fruchter et al. 1990), B1744–24A (Lyne et al. 1990, Nice & Thorsett 1992) and J2051–0827 (Stappers et al. 1996), all having companions of mass $M_c < 0.10 M_\odot$, the eclipses are believed to be caused by a wind resulting from ablation of the companion by a relativistic pulsar wind. PSR J1740–5340 is in a wide orbit and the wind energy density impinging on the companion is significantly less than that estimated for the close eclipsing systems, and is unlikely to drive a wind of sufficient density off a degenerate companion. In the discovery paper, D'Amico et al. (2001) argued that the companion could be an unevolved star of mass comparable to the turnoff mass of the cluster, $\sim 0.8 M_\odot$, releasing a wind sufficiently dense to produce the observed eclipses. Such a hypothesis, which would make PSR J1740–5340 an unusual system, can be ultimately tested with the optical identification of the pulsar companion.

In this Letter we report on the first year of pulse timing observations of this pulsar. We provide timing parameters, including the position, and we report on further observational evidence of the interaction of the pulsar signal with the companion atmosphere.

2. OBSERVATIONS AND RESULTS

Regular timing observations have been made since 2000 July with the Parkes radio telescope, using the center beam of the multibeam receiver at 1.4 GHz. The observing system is the one used in the discovery observations (D'Amico et al. 2001). The effects of interstellar dispersion are minimized with a filter

bank having 512×0.5 MHz frequency channels for each of two linear polarizations. After detection, the signals from individual channels are added in polarization pairs, integrated, 1 bit-digitized every 125 μ s, and then recorded on magnetic tape. Pulse times of arrival (TOAs) are determined offline by fitting a standard pulse profile having a high signal-to-noise ratio to the observed profiles and analyzed using the program TEMPO¹ and the DE200 solar system ephemeris (Standish 1982). A simple Keplerian model of a binary system was used in the analysis.

For about six months we routinely collected data on this pulsar several times a week using an integration time of 30 min for each observation. From the orbital parameters obtained during the confirming observations in 2000 July, we knew that the pulsar was eclipsed in the orbital phase interval 0.05–0.45, so we have generally made observations at epochs when the predicted orbital phase was outside this interval. In this way we have obtained a reasonable number of good quality integrated pulse profiles (with signal-to-noise ratios in the range 10–25 and typical timing errors in the range 10–40 μ s), while some low quality profiles were rejected. Most of the latter were obtained at epochs relatively close to the predicted eclipse edge, but some were taken far from the nominal eclipse region, at orbital phases where the pulsar was expected to be detected clearly. We also noted that, while we could obtain a coherent timing solution over several months, the resulting post-fit rms scatter of the residuals was large compared to the typical nominal timing uncertainties of individual TOAs, suggesting the presence of systematic effects.

In order to probe the hypothesis that this behavior could be due to the interaction of the pulsar radiation with the companion atmosphere, we have recently initiated a series of long observations starting close to the eclipse edge near the descending node, and lasting for a substantial fraction of the orbit in the non-eclipsing region.

¹<http://pulsar.princeton.edu/tempo>.

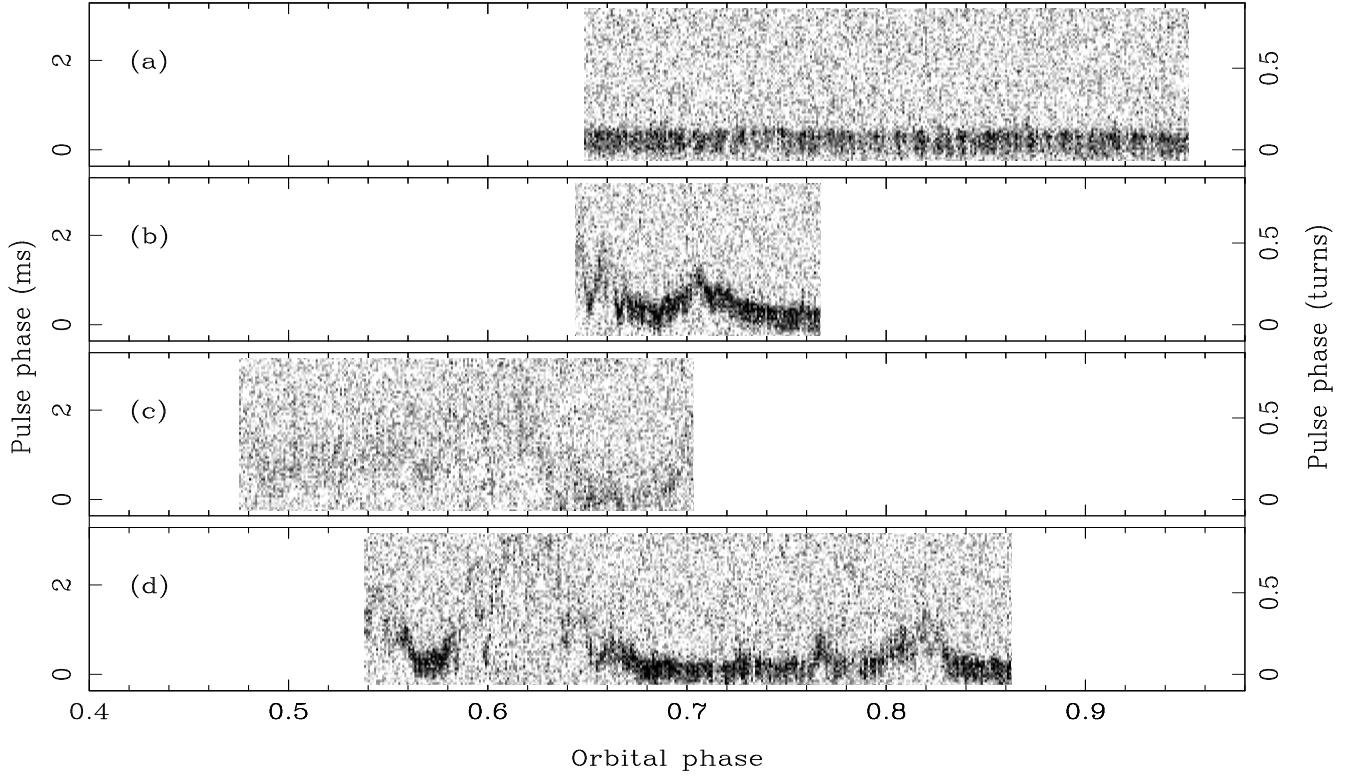


Fig. 1.— Observed signal intensity at 1.4 GHz as a function of orbital phase and pulsar phase for four long observations away from the nominal eclipse region. The data are processed in contiguous integrations of 120 s duration. (a) ~ 10 hr observation starting on 2000 December 3 at 22:23 UT; (b) ~ 4 hr observation starting on 2001 March 1 at 22:32 UT; (c) ~ 7 hr observation starting on 2001 March 5 at 18:31 UT; (d) ~ 11 hr observation starting on 2001 March 12 at 15:02 UT.

The orbital period is ~ 32 hr and the pulsar is visible at Parkes for ~ 11 hr on a given day. Thus far we have obtained four relatively long observations. The results are shown in Figure 1. In one case (Fig. 1a) the pulsar signal was relatively stable in intensity and pulse phase, while in the other three cases (Figs. 1b, c and d) significant excess propagation delays of up to ~ 3 ms and strong intensity variations are observed. In particular, in the case of Figure 1c, the pulsar signal was always rather weak and the pulse was about two times wider than usual, covering about 30–50% of the rotational phase. The correlation between delay peaks and flux reduction suggests that interstellar scintillation is not responsible for this behavior. These fluctuations are comparable to those observed at a lower frequency (~ 400 MHz) in PSR B1957+20 near the eclipse edges around orbital phases 0.2 and 0.3 (Fruchter et al. 1990). In PSR J2051–0827 (Stappers et al. 1996) flux density variations and variable propagation delays are seen at 1.4 GHz when the pulsar signal is detectable through the eclipse region. PSR B1744–24A displays similar irregularities also far from the usual eclipse region, with typical delays of $\sim 300 \mu\text{s}$ (Nice & Thorsett 1992). Instead, much larger excess delays, $\gtrsim 1$ ms, are observed at nearly all orbital phases in the case of PSR J1740–5340. These observations suggest that the pulsar is in fact orbiting within an extended envelope of matter released from the companion.

We investigated the frequency-dependent behavior of the observed delay events by splitting the 256-MHz bandwidth available at 1.4 GHz into two adjacent subbands. As can be seen from Figure 1, significant pulse broadening and signal-to-noise reduction is usually associated with large delays. We have therefore limited our analysis to small delays only. Figure 2 shows an example of the measured excess delays in the two

subbands. The small panel also shows these measurements plotted against each other. The best-fitting straight line corresponds to $\Delta t \propto \nu^{-2.02 \pm 0.30}$ for the excess delays, consistent with the ν^{-2} dependency expected if the delays are due to dispersion in an ionized medium. If entirely due to dispersion, the excess propagation delays of up to ~ 3 ms visible in Figure 1 would correspond to electron column density variations of $\sim 1.5 \times 10^{18} \Delta t_{-3} \text{ cm}^{-2}$, or $\Delta \text{DM} \sim 0.47 \Delta t_{-3} \text{ cm}^{-3} \text{ pc}$ (Δt_{-3} being the delay at 1.4 GHz in ms). This corresponds to a pulse broadening of $0.10 P \Delta t_{-3} = 0.36 \Delta t_{-3} \text{ ms}$ over the receiver bandwidth (to be compared with an intrinsic pulse FWHM of $0.17 P$) and may be responsible for most of the signal attenuation and pulse broadening observed near the delay peaks.

From Figure 1 we can also see that far from the eclipse region the typical time scale of the rise to maximum delay is of order 1–2 hr. This indicates that observations of $\gtrsim 3$ hr are required in order to identify reliably a non-delayed portion of an observation and to obtain a bona fide TOA. This explains why a timing solution mainly based on relatively short integrations may be affected by systematic effects.

In order to obtain a reliable phase-connected timing solution for this pulsar we have selected by visual inspection among all the data collected at 1.4 GHz in the last 12 months only those TOAs with no indication of delay and those corresponding to profiles not affected by pulse broadening. In this way we have obtained a solution with a post-fit rms residual of $\sim 120 \mu\text{s}$. The corresponding model parameters are reported in Table 1. Figure 3a shows the residuals for all TOAs collected whereas Figure 3b shows those for the selected TOAs only, all relative to the model in Table 1. The dispersion measure (DM) was fitted using TOAs from two adjacent subbands from the stable long integration shown in Figure 1a. A fit for orbital ec-

centricity may be biased because only $\sim 60\%$ of the orbit is sampled. Nevertheless a formal fit results in an upper limit of $e < 10^{-4}$ (3σ), and in deriving the parameters listed in Table 1 we have fixed $e = 0$. Further observations may better constrain this limit. Similarly, a longer data span will be needed for investigating possible changes in the orbital parameters, as seen e.g. in PSR B1957+20 (Nice, Arzoumanian & Thorsett 2000).

3. DISCUSSION

PSR J1740–5340 has the longest orbital period (32 hr) and the most massive minimum companion mass ($0.19 M_{\odot}$, assuming a neutron star mass of $1.40 M_{\odot}$) among the 10 known eclipsing pulsars (Nice, Arzoumanian & Thorsett 2000; Camilo et al. 2000). When combined with the typical duration of the eclipse at 1.4 GHz (~ 13 hr), these parameters imply an eclipse radius R_E larger than the orbital separation a for any value of the orbital inclination i . R_E is defined as the chord subtended on the orbital circumference of radius a by the angle between the orbital phase of eclipse ingress (or egress) and the orbital phase 0.25. Table 2 shows the relevant parameters associated with different companion types: a $0.19 M_{\odot}$ He-white dwarf (WD) (corresponding to $i = 90^\circ$) and a range of main sequence (MS) stars spanning the mass interval $M_{ms} \sim 0.19 - 0.8 M_{\odot}$ (the latter value being the maximum compatible with the age of NGC 6397). As can be seen, $R_E \sim 7.5 R_{\odot} > a \sim 6.5 R_{\odot}$.

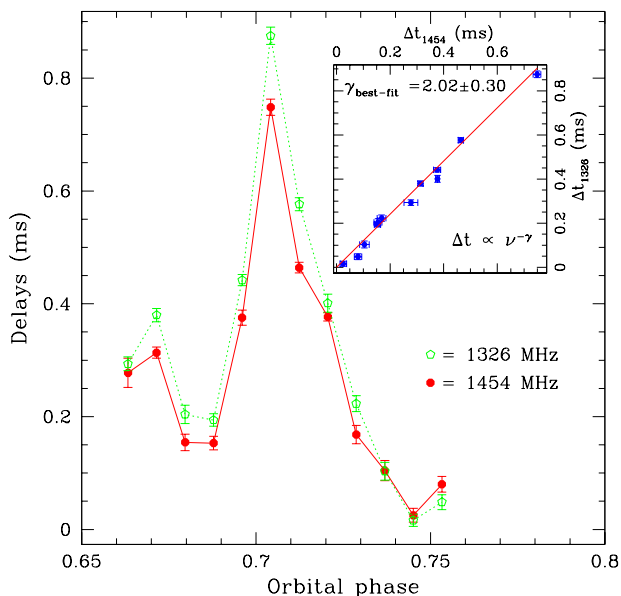


Fig. 2.— Excess group delays measured in two 128 MHz-wide bands centered at 1454 MHz (filled symbols, connected by a solid line) and at 1326 MHz (open symbols, connected by a dotted line) for an event occurring at orbital phases 0.65–0.75 on 2001 March 1 (see Fig. 1b). The delays in the two sub-bands are fitted (inserted panel) with a straight line of slope 1.21 ± 0.04 , corresponding to a frequency dependence for the delays ($\Delta t \propto \nu^{-\gamma}$) with a best-fit power-law index $\gamma = 2.02 \pm 0.30$.

From the observation in Figure 1a, we infer that there are no systematic electron column density variations over a wide orbital phase interval. Hence the neutron star is not orbiting inside a steady corona of ionized matter surrounding the companion star. More likely, the pulsar is just skimming a large envelope of matter, whose clumpiness and varying shape at distances from the companion comparable with R_E could be triggered by

the movement and the energy flux of the pulsar itself. The irregular features appearing in the three observations of 2001 March (Figs. 1b–1d) could for example represent this kind of interaction.

The values of the Roche lobe radius R_L span the interval $1.3 - 2.2 R_{\odot}$ (Eggleton 1983). Because $R_E > a > R_L$, the matter causing the eclipses escapes the gravitational influence of the companion star and therefore must be continuously replenished. The large position offset of PSR J1740–5340 with respect to the center of NGC 6397 ($r \sim 0'.55$) limits the unknown contribution to the observed period derivative \dot{P} due to acceleration in the globular cluster potential. Assuming a King model (1962) for the central mass density, core radius $r_c = 0'.05$ and central luminosity density (in units of L_{\odot}/pc^3) $\log(\rho_L[0]) = 5.6$ (Harris 1996), distance $d = 2.6$ kpc (Reid & Gizis 1998), and a mass-to-luminosity ratio $M/L = 3.3$ (Pryor & Meylan 1993), we derive (see e.g. Camilo et al. 2000) $|\dot{P}_{\text{acc}}| < 4\pi G/(9c)(r_c/r)r_c d(M/L)\rho_L(0)P \sim 10^{-20}$. Even accounting for the uncertainties in some of the above parameters (e.g., r_c), the observed \dot{P} (Table 1) should be only slightly affected by \dot{P}_{acc} . Thus we can use \dot{P} to infer the rotational energy loss of the pulsar, $\dot{E} \sim 1.4 \times 10^{35}$ ergs s^{-1} . A He-white dwarf of minimum mass $M_{wd} = 0.19 M_{\odot}$ with an effective temperature $T_{wd} = 10^4$ K has radius $R_{wd} = 0.033 R_{\odot}$ (Driebe et al. 1998, Serenelli et al. 2001). Because the radius decreases with increasing temperature, we use R_{wd} as an upper limit. At the distance of $6.0 R_{\odot}$, the power impinging on the degenerate companion would be $W_{wd} \lesssim 10^{30}$ ergs s^{-1} . This would allow release of an ionized wind from the degenerate companion at a maximum rate $\dot{M}_{wd,max} = W_{wd}(R_{wd}/GM_{wd}) \lesssim 1.6 \times 10^{-12} M_{\odot} \text{y}^{-1}$.

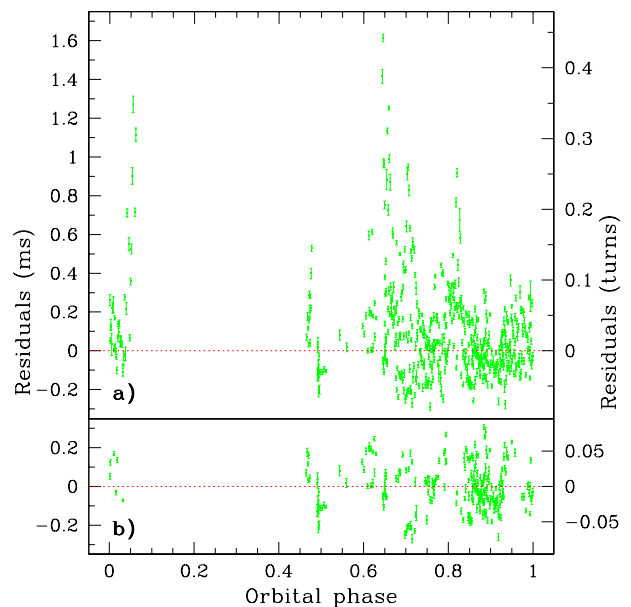


Fig. 3.— (a) Timing residuals of all the TOAs collected (525 points derived from 46 observations of length ranging from ~ 30 min up to ~ 11 hr) relative to the timing model in Table 1. (b) Timing residuals of the 241 TOAs used to derive the phase-connected solution reported in Table 1. The scales of the two panels are identical. The post-fit timing residuals in panel b, while smaller on average than those in panel a, are still noticeably large compared to the nominal TOA uncertainties. This effect may be caused by small-scale electron density fluctuations not modeled in our present fits.

Assuming isotropic emission, mass continuity implies that the companion star releases mass at a rate $\dot{M}_c = 4\pi R_E^2 \rho(R_E) v_f$.

Using the values in Table 2 and the density at the eclipse radius inferred from the observation of the excess delays assuming completely ionized matter ($\rho[R_E] \sim 3 \times 10^{-18} \Delta t_{-3} \text{ g cm}^{-3}$), we obtain $\dot{M}_c \sim 1.5 \times 10^{-11} \Delta t_{-3} v_{f,8} M_\odot \text{ y}^{-1}$ where $v_{f,8}$ is the wind velocity at R_E in units of 10^8 cm s^{-1} (typical order of magnitude of the escape velocity from the surface of the companion). Thus, only in the case of low terminal velocity of the wind ($v_f \lesssim 100 \text{ km s}^{-1}$, corresponding to improbable electron temperatures of $\lesssim 200 \text{ K}$ at R_E) could the pulsar flux sustain the ablation. More massive WDs would further exacerbate these difficulties.

The hypothesis of a MS companion appears more viable: such a companion could have been acquired as a result of an exchange interaction in the cluster core (Sigurdsson & Phinney 1993; Heggie, Hut & McMillian 1996), a scenario possibly supported also by the position of PSR J1740–5340 ~ 11 core radii from the center of NGC 6397. This object is the second farthest pulsar from a cluster core (in units of core radii) among the 36 pulsars in globular clusters with precisely determined positions (after PSR B2127+11C in M15, located at ~ 13 core radii).

The unperturbed radius R_{ms} of a MS star of mass $M_{ms} \sim 0.19\text{--}0.8 M_\odot$ is $\sim 6\text{--}30$ times greater than the maximum possible radius for a WD (Table 2). The energy required for transporting a unit mass from the surface of the companion to its Roche lobe radius $R_{L,*}$ is $U_* \sim GM_*(R_*^{-1} - R_{L,*}^{-1})$. Given this, the corresponding maximum ablation rate for a MS companion is $\dot{M}_{ms,max} \sim (R_{ms}/R_{wd})^2 (U_{wd}/U_{ms}) \dot{M}_{wd,max} \sim 200\text{--}6000 \dot{M}_{wd,max} = (3\text{--}90) \times 10^{-10} M_\odot \text{ y}^{-1}$. Therefore, only 0.2–5% of the impinging power would be needed to sustain the inferred mass loss rate \dot{M}_c . The bulk of the pulsar energy would thus be available for heating the companion photosphere and perhaps inflating its radius up to Roche lobe, in turn making the release of the wind even easier. This model should be more easily applicable to a light MS star, as large convective envelopes favor bloating of

the star (Podsiadlowski 1991).

Another hypothesis for explaining the large mass loss rate \dot{M}_c is that the companion is an evolved star that spun up the millisecond pulsar and that is presently undergoing the presumed final stages of mass loss. In this case, mass accretion and spinning up of the pulsar would now be inhibited by the pulsar wind flux which could expel the matter overflowing from the Roche lobe of the companion (see for instance Burderi et al. 2001 and references therein). If substantiated, this would be the first confirmed example of a recently born millisecond pulsar. The apparent rather young spin-down age of PSR J1740–5340 ($\tau_c = P/2\dot{P} \sim 350 \text{ Myr}$, assuming as mentioned earlier that \dot{P}_{acc} is negligible), and its surface magnetic field ($B = 3.2 \times 10^{19} [P\dot{P}]^{1/2} \sim 8 \times 10^8 \text{ G}$) would support this model. However, the future evolution of the binary (companion evolving into a WD?) remains unclear. Detailed simulations of the system are required for comparing this or other more exotic scenarios (Burderi, D’Antona & Burgay 2001, in preparation) with the parameters derived from radio and optical observations.

Ferraro et al. (2001) report the possible identification of the optical companion to PSR J1740–5340 with a bright variable star and Grindlay et al. (2001) have detected with *Chandra* the X-ray counterpart of the millisecond pulsar. The availability of data in a large spectral band, from radio to optical and X-rays, should help understanding this exotic system and the mechanism(s) responsible for the radio eclipses.

The Parkes radio telescope is part of the Australia Telescope which is funded by the Commonwealth of Australia for operation as a National Facility. We thank the staff at Parkes for their support of this project, and L. Burderi for carefully reading the manuscript and for stimulating discussions. N.D’A. and A.P. are supported by the Ministero della Ricerca Scientifica e Tecnologica (MURST). F.C. is supported by NASA grant NAG5-9095.

REFERENCES

- Burderi, L. et al. 2001, in *Evolution of Binary and Multiple Star Systems*, ed. P. Podsiadlowski, S. Rappaport, A. King, F. D’Antona, & L. Burderi (San Francisco: ASP), 229, 455, astro-ph/0104170
- Camilo, F., Lorimer, D. R., Freire, P., Lyne, A. G., & Manchester, R. N. 2000, *ApJ*, 535, 975
- D’Amico, N., Lyne, A. G., Manchester, R. N., Possenti, A., & Camilo, F. 2001, *ApJ*, 548, L171
- Driebe, T., Schonberner, D., Blocker, T., & Herwig, F. 1998, *A&A*, 339, 123
- Eggleton, P. P. 1983, *ApJ*, 268, 368
- Ferraro, F., Possenti, A., D’Amico, N., & Sabbi, E. 2001, *ApJL*, this issue
- Fruchter, A. S. et al. 1990, *ApJ*, 351, 642
- Grindlay, J. E., Heinke, C. O., Edmonds, P. D., Murray, S. & Cool, A. 2001, *ApJL*, submitted
- Harris, W. E. 1996, *AJ*, 112, 1487
- Heggie, D. C., Hut, P., & McMillian, S. L. W. 1996, *ApJ*, 467, 359
- King, I. 1962, *AJ*, 67, 471
- Lyne, A. G. et al. 1990, *Nature*, 347, 650
- Nice, D. J., Arzoumanian, Z., & Thorsett, S. E. 2000, in *Pulsar Astronomy - 2000 and Beyond*, IAU Colloquium 177, ed. M. Kramer, N. Wex, & R. Wielebinski, (San Francisco: ASP), 67
- Nice, D. J. & Thorsett, S. E. 1992, *ApJ*, 397, 249
- Pryor, C. & Meylan, G. 1993, in *Structure and Dynamics of Globular Clusters*, ed. S. G. Djorgovski and G. Meylan, (San Francisco: ASP), 357
- Podsiadlowski, P. 1991, *Nature*, 350, 136
- Reid, I N., & Gizis, J. E. 1998, *ApJ*, 116, 2929
- Serenelli, A. M., Althaus, L. G., Rohrmann, R. D., & Benvenuto, O. G. 2001, *MNRAS*, 325, 607
- Sigurdsson, S., & Phinney, E.S. 1993, *ApJ*, 415, 631
- Standish, E. M. 1982, *A&A*, 114, 297
- Stappers, B. W. et al. 1996, *ApJ*, 465, L119

TABLE 1
PARAMETERS OF THE PSR J1740–5340 SYSTEM

Parameter	Value
Right Ascension (J2000)	17 ^h 40 ^m 44 ^s .589(4)
Declination (J2000)	–53° 40′ 40″.9(1)
Galactic longitude, l	338° 164
Galactic latitude, b	–11° 96
Dispersion Measure, DM (cm ^{–3} pc)	71.8(2)
Period, P (s)	0.00365032889720(1)
Period derivative, \dot{P} (10 ^{–20})	16.8(7)
Period epoch (MJD)	51917.0
Orbital period (d)	1.35405939(5)
Projected semimajor axis (s)	1.65284(7)
Epoch of ascending node, T_{asc} (MJD)	51749.710822(6)
Eccentricity ^a , e	< 10 ^{–4}
Data span (MJD)	51719–52116
Post-fit rms (μ s)	114
Mass function (M_{\odot})	0.0026442(3)
Companion mass, M_c (M_{\odot})	> 0.19

NOTE.—Numbers in parentheses represent three times the formal 1σ uncertainties given by TEMPO in the least-significant digits reported.

^aAll other parameters have been derived setting $e = 0$ (see text).

TABLE 2
PARAMETERS FOR POSSIBLE COMPANION

Parameter	He-WD	MS
Companion mass, M_c (M_{\odot})	0.19	0.19–0.8
Orbital inclination, i (°)	90	90–17
Orbital separation, a (R_{\odot})	6.0	6.0–6.7
Roche lobe radius, R_L (R_{\odot})	1.3	1.3–2.2
Eclipse radius, R_E (R_{\odot})	7.1	7.1–7.9
Stellar radius, R (R_{\odot})	~ 0.03	0.2–0.96